Progress In Electromagnetics Research C, Vol. 56, 55–64, 2015

Multiband Circularly Polarized Stacked Microstrip Antenna

Dinesh K. Singh[1], Binod K. Kanaujia[2, *], Santanu Dwari[1], Ganga P. Pandey[3], and Sandeep Kumar[1]

Abstract—In this paper, a multiband circularly polarized capacitive coupled stacked microstrip antenna is proposed. The multiband circular polarization (CP) is achieved by corner truncation, embedding slits and inclined slots on a three layered antenna structure. The proposed antenna also shows wideband behavior with an impedance bandwidth of 52.13% in the frequency range of 4.85 GHz to 8.27 GHz, while 3 dB axial ratio bandwidths in five CP bands are 0.51%, 4.54%, 0.33%, 0.83% and 1.29% in the frequency range of 5.12 GHz to 5.15 GHz, 5.45 GHz to 5.70 GHz, 5.90 GHz to 5.92 GHz, 6.25 GHz to 6.31 GHz and 7.68 GHz to 7.78 GHz, respectively. The antenna prototype is fabricated, and simulated results as axial ratio, radiation pattern and the reflection coefficient are validated with measured result.

1. INTRODUCTION

Recently, the multiband circularly polarized microstrip antennas are in great demand in current wireless communication system because they overcome the problems of mutual coupling and negative effect on the overall system performance caused by integrating the multiple circularly polarized antennas to cover the different frequency bands. Also, the circularly polarized antennas have the advantage of better mobility, better orientation between transmitter and receiver and better weather penetration than linearly polarized antennas [1]. It is, therefore, of great interest to design a single antenna that can facilitate multiband circular polarization. The satellite communication systems perform better in C-band (4–8 GHz) than in Ku band (11.2–14.5 GHz) under adverse weather conditions. The single-feed and dual-feed techniques are the common techniques used to design the circularly polarized microstrip antennas. Due to the simple structure, single feed antennas are receiving more attention than the dual-feed technique, which uses an external polarizer and make the antenna structure complex. In [2], a broad band circular polarization (CP) is achieved by using dual capacitively coupled feeds and a Wilkinson power divider having 90° phase shift between its two output feed lines. But the dual feed makes the antenna structure complex. The CP antenna using a single feed with two stacked patches uses S-shaped impedance matching network [3] to generate circularly polarized band and impedance band which coincide. The circular polarization is obtained by the upper parasitic patch rotating 90° sequentially based on the lower patch and truncating corners. As explained in [4], the circular polarization is achieved by embedding an arrowhead-shaped slot in the first quadrant along the diagonal axis of the square patch which makes the antenna structure asymmetric. In [5], four slots are etched near edges of the patch and a crossed slot etched in the centre of the patch for generating dual CP operation. In [6], a circular radiating patch with a ring slot, two substrates with an air layer sandwiched between them and a capacitive coupled feed is proposed. The dual CP radiation is obtained by introducing a pair of stubs and ring slot. Several designs of stacked microstrip antenna to achieve dual CP operation have recently

Received 11 December 2014, Accepted 2 February 2015, Scheduled 5 February 2015

* Corresponding author: Binod Kumar Kanaujia (bkkanaujia@ieee.org).

[1] Department of Electronics Engineering, Indian School of Mines, Dhanbad, Jharkhand 826004, India. [2] Department of Electronics & Communication Engineering, AIACTR, Delhi 110031, India. [3] Department of Electronics & Communication Engineering, Maharaja Agrasen Institute of Technology, Delhi 110085, India.

been reported [7–12]. In a stacked structure; the feed is connected to only one patch while patches on the other layers receive the excitation from the fed patch. Stacked patches can be either used for multiband or wideband operation as far as impedance bandwidth is concerned. Moreover, stacked patches have extra degree of freedom in case of operating band selection, and have independent control of resonant frequencies. In the recent years, stacked structure has emerged as a technique to implement multiband CP antenna. By keeping impedance bandwidth of each layer patch wide, the various layers can be made to operate to provide one CP band and each layer is responsible for individual CP band. While if each layer is designed to provide more than one CP band and has wideband behavior, the number of required layers can be reduced. By integrating dual-feed patch antennas with a branch line coupler in a multilayer structure, the dual CP characteristic is obtained in [7]. Here, at the cost of complex structure due to multilayer and dual feed, good CP bandwidth is obtained. In [8], the design of a dual circularly polarized multilayer microstrip antenna element fed by a gap coupled probe has been presented. The 3 dB axial ratio bandwidth of 2% and 1.5% in the two bands was obtained. Stacked microstrip antenna with dual-band CP behavior is presented in [9]. The dual CP has been realized by combining the stacked configuration with a truncated edge technique at its top and lower patches. In [10], two miniaturized radiation elements using folded structures are stacked vertically to obtain dual CP band. In both CP bands, the 3-dB axial ratio is around 1%. In [11], a dual-band circularly polarized single feed microstrip antenna is presented. The dual CP radiations are achieved by introducing a protruding semi ellipse on the edge of the patch and multilayer substrates between ground planes and radiating patch. The stacked patch antenna with dual-band CP is presented in [12]. The dual CP radiations are achieved by embedding two pairs of narrow slots. In [13], a single layer feed is used to excite a single square patch integrated with a novel asymmetrical slot and two differently truncated corners to achieve dual-band CP. Triple band CP operation by using a four element trap loaded inverted L-antenna array is realized in [14]. The structure of the antenna is complex due to inverted L-antenna array. Aperture coupled two stacked patches are used to achieve a triple band circular polarization operation [15]. But; the antenna is fed by two feed lines having 180° phase difference. In [16], by inserting two pairs of narrow slots parallel to the edges of the top square patch and cutting slits in the bottom square patch, triple band CP radiation is achieved. In [17], three stacked patches with a slit and I-slot have been used to achieve three circularly polarized bands. In [18], the four stacked patches are used to achieve the quad band circular polarization.

In this paper, wideband capacitive coupled stacked patch antenna with multiband CP operation is presented. The multiband CP operation is achieved by corner truncation, cutting slits in the three stacked patches, and introducing inclined slots on the middle patch and lower patch. The proposed antenna gives five different CP bands with the axial ratio bandwidth of 0.51%, 4.54%, 0.33%, 0.83% and 1.29%. The effect of size of slits, slots and corner truncation is studied in detail since they have a significant effect on the CP performance of the proposed antenna. The antenna is applicable for satellite communication, some Wi-Fi services (5.47 GHz to 5.725 GHz for HIPERLAN/2), some cordless phone services and some weather radar systems. The detailed analysis is carried out in the following sections.

2. ANTENNA DESIGN

The schematic and fabricated structures of the proposed antenna with capacitive coupled feeding arrangement are shown in Figure 1 and Figure 2, respectively. The antenna consists of three stacked rectangular patches of dimension $L \times W$ with centers of all the patches aligned. All the three patches are corner truncated by same dimension of $\Delta L \times \Delta L$ to generate a CP radiation pattern. The first two patches are etched on the upper and lower surfaces of the substrate RT Duroid RO3003 with $\varepsilon_r = 3.0$ and thickness $h_1 = 1.6$ mm. The third patch is etched on the lower surface of the foam material with $\varepsilon_r = 1.06$ and thickness $h_2 = 1.6$ mm. On the upper conducting patch, two horizontal slits having lengths L_1 and L_2 are cut at $w_1 = 1.7$ mm from the left upper and right lower corners of the patch. On the middle patch, a slit of length L_3 is cut at w_1 from the left upper corner of the patch and a slot of length L_4 is introduced at the center of the middle patch at an angle of 135°, while on the lower patch, two parallel slots of lengths L_6 and L_7 are embedded at an angle of 45° at the centre and at the distance of d_1 from the centre respectively. The slit of length L_5 is cut at w_1 from the left upper corner of the lower path. All the slits and inclined slots have the same width ($w = 1$ mm). Two slits in the

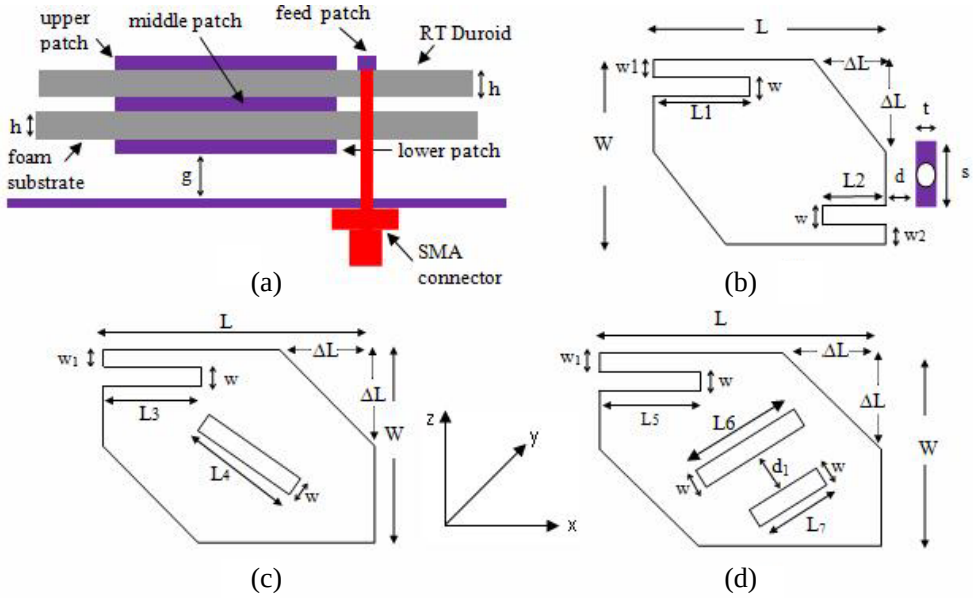

Figure 1. Geometry of the proposed multiband CP antenna, (a) side view and top views of (b) upper patch, (c) middle patch, (d) lower patch.

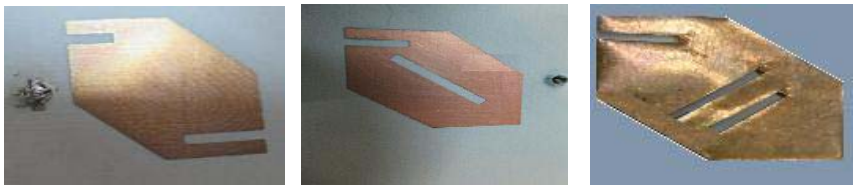

Figure 2. Fabricated prototype of the proposed antenna, (a) upper patch, (b) middle patch, (c) lower patch.

upper patch make the antenna dual-band circularly polarized, while the slits and inclined slot in the middle patch add two more CP bands. The slit and inclined slots are embedded in the lower patch to generate fifth CP band. The upper patch is capacitively coupled through a feed strip of dimension $t \times s$ which is printed on the upper surface of the substrate RT Duroid RO3003 and is connected to a SMA connector, via holes in foam material and RT Duroid substrate, while the lower and middle patches are electromagnetically coupled. The gap between the feed strip and upper patch is $d = 2.12\,\text{mm}$. The antenna is suspended above the ground plane at $g = 4.44\,\text{mm}$.

3. PARAMETRIC STUDIES

The multiband CP antenna is able to operate at different frequency bands on a single antenna and can be useful for several applications. Hence, the optimization goal is to obtain multiple CP bands with good axial ratio bandwidth. The parametric study in terms of its various controlling elements is carried out to obtain optimal values. All simulations are carried out using IE3D$^{\text{TM}}$. The size of the slits, inclined slots and corner truncation are varied to obtain the optimal goal and to understand the effect of these parameters on the resonant frequency and an axial ratio of the antenna. In the parametric variation, only one parameter is considered at a time, while the others are kept constant. It has been observed that slit's lengths L_1, L_2, L_3 and L_5, corner truncation length ΔL, slot's lengths L_4, L_6 and L_7 have no significant effect on the reflection coefficient for the given variation. Hence, the effect of parametric variation in the axial ratio is presented in the following section.

3.1. Effect of Slit's Length

Figure 3 shows the effect of the slit length L_1 of the upper patch on the axial ratio of the antenna. When the slit length L_1 decreases, the three CP bands are obtained. Five CP bands are obtained with an increase in slit length L_1, but 3 dB axial ratio bandwidth of the third CP band decreases. It is realized that the optimum value is obtained at $L_1 = 6.74$ mm with five CP bands. Figure 4 shows the effect of the slit length L_2 of the upper patch on the axial ratio of the antenna. It can be seen from the figure that four CP bands are obtained with a decrease in slit length L_2, while five CP bands are obtained with an increase in slit length L_2. The effect of the slit length L_3 of the middle patch on the axial ratio of the antenna is shown in Figure 5. It can be easily observed that, with a decrease or increase in slit length L_3, four CP bands are achieved. The best CP performance is obtained with $L_3 = 5.95$ mm having five different CP bands. The effect of the slit length L_5 of the lower patch on the axial ratio of the antenna was also studied, but had the minor effect on the axial ratio as shown in Figure 6.

Table 1 summarizes the effect on centre frequencies (CF) and axial ratio bandwidth (ARBW) of different CP bands of the antenna with variation in the slit's length. The CF of CP bands AR1, AR2, AR3 and AR4 shifted downward and no effect is observed on CF of AR5 with increase in the slit length L_1. The ARBW of CP band AR2 is decreased. With the decrease in the slit length L_1, the CP bands AR1 and AR4 disappear and three CP bands AR2, AR3 and AR5 are obtained. It can be observed that decreasing the slit length L_1 has great effect on CP performances. The CP band AR4 disappeared

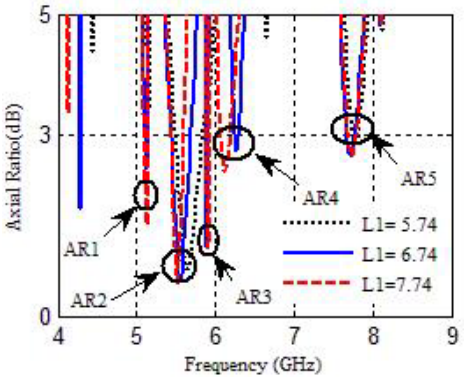

Figure 3. Variation of axial ratio for different values of length L_1 of slit in upper patch.

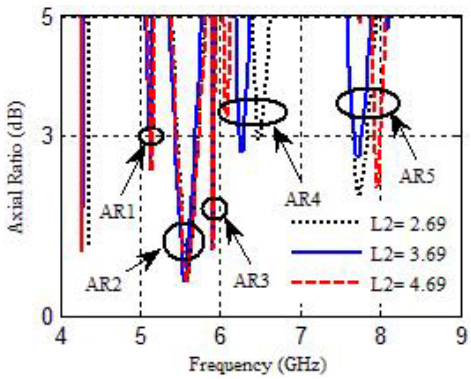

Figure 4. Variation of axial ratio for different values of length L_2 of slit in upper patch.

Table 1. Summary of results presented in Figures 3–6.

Parameter	Slit length (mm)	AR1		AR2		AR3		AR4		AR5	
		CF (GHz)	ARBW (%)	CF (GHz)	ARBW (%)	CF (GHz)	ARBW (%)	CF (GHz)	ARBW (%)	CF (GHz)	ARBW (%)
L_1	7.74	5.115	0.97	5.51	2.90	5.895	0.500	6.12	1.96	7.730	1.293
	6.74	**5.135**	**0.58**	**5.575**	**4.484**	**5.910**	**0.338**	**6.280**	**0.955**	**7.730**	**1.293**
	5.74	NA		5.655	6.189	5.910	0.338	NA		7.770	0.772
L_2	4.69	5.135	0.58	5.585	4.834	5.910	0.338	NA		7.965	0.878
	3.69	**5.135**	**0.58**	**5.575**	**4.484**	**5.910**	**0.338**	**6.280**	**0.955**	**7.730**	**1.293**
	5.69	5.145	0.38	5.615	5.520	5.910	0.338	6.485	0.462	7.745	2.194
L_3	5.95	5.115	1.36	5.501	4.000	5.910	0.338	NA		7.345	2.859
	4.95	**5.135**	**0.58**	**5.575**	**4.484**	**5.910**	**0.338**	**6.280**	**0.955**	**7.730**	**1.293**
	3.95	NA		5.640	4.964	5.910	0.338	6.295	1.429	8.205	1.340
L_5	7.0	5.13	0.38	5.570	4.667	5.825	0.515	6.270	0.637	7.735	1.680
	6.0	**5.135**	**0.58**	**5.575**	**4.484**	**5.910**	**0.338**	**6.280**	**0.955**	**7.730**	**1.293**
	5.0	5.14	0.77	5.575	4.484	5.925	0.168	6.280	0.955	7.735	1.422

and CF of CP band AR5 shifted upward with an increase in the slit length L_2. The centre frequencies of all the CP bands shifted upward with decreasing the slit length L_2. The CP band AR1 disappeared and CF of CP band AR5 shifted upward with decreasing the slit length L_3, while with increasing the slit length L_3 the CP band AR4 disappeared and CF of CP band AR5 shifted downward. There is a little effect on all CP bands with increasing and decreasing the slit length L_5.

3.2. Effect of Slot's Length

In this section, the variation of slot's length on the CP performances is studied. The variation of axial ratio for different values of length L_4 of the slot in the middle patch is illustrated in Figure 7. When decreasing slot length L_4, three CP bands are obtained and with an increasing slot length, five CP bands are obtained. The optimized value of this parameter is obtained at $L_4 = 10\,\text{mm}$. Figure 8 shows the axial ratio of the antenna with different values of slot length L_6. A significant effect is observed on CP bands with a variation of the slot length L_6. Four distinct CP bands are obtained by decreasing or increasing the slot length L_6. The optimized value is obtained at $L_6 = 10\,\text{mm}$ with five CP bands. The effect of the different value of length L_7 of slot in lower patch on axial ratio is illustrated in Figure 9. From tuning the length of slot L_7, it is seen from the figure that it has no significant effect on the axial ratio. Five different CP bands are achieved with increasing or decreasing the slot length L_7.

Table 2 summarizes the effect on the CF and ARBW of different CP bands of the antenna with variation in the slot's length. The CF of CP bands AR1 and AR4 shifted downward, and CF of CP bands AR2, AR3 and AR5 shifted upward by increasing the slot length L_4. From the table, it is observed that decreasing the slot length L_4 deeply affects the CP bands of the antenna and only three CP bands, i.e., AR2, AR3 and AR5 are obtained. The CF of CP AR3 and CP band AR5 shifted upward with decreasing and increasing the length L_6, respectively. By increasing and decreasing the slot length L_7, only CP band AR3 is affected. The CF of CP band AR3 shifted downward and upward with increasing and decreasing the slot length, respectively.

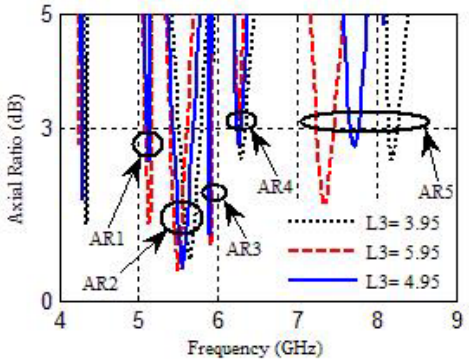

Figure 5. Variation of axial ratio for different value of length L_3 of slit in middle patch.

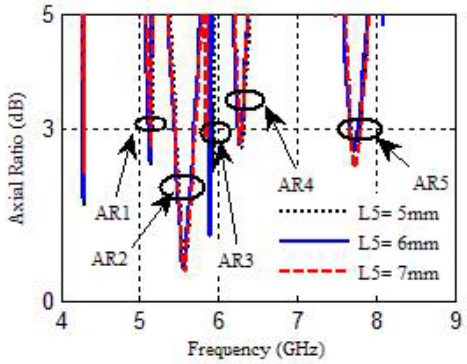

Figure 6. Variation of axial ratio for different value of length L_5 of slit in lower patch.

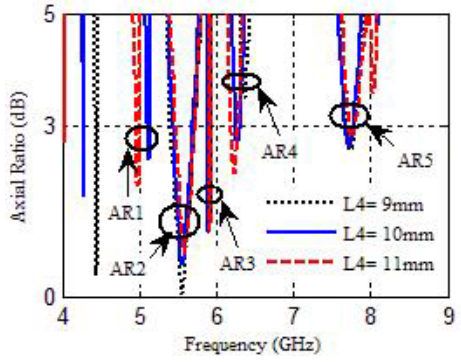

Figure 7. Variation of axial ratio for different value of length L_4 of slot in lower patch.

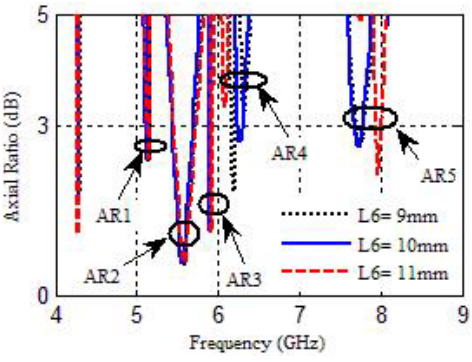

Figure 8. Variation of axial ratio for different value of length L_6 of slot in lower patch.

Table 2. Summary of results presented in Figures 7–9.

parameter	Slot length (mm)	AR1		AR2		AR3		AR4		AR5	
		CF (GHz)	ARBW (%)	CF (GHz)	ARBW (%)	CF (GHz)	ARBW (%)	CF (GHz)	ARBW (%)	CF (GHz)	ARBW (%)
L_4	11	4.975	0.904	5.585	4.476	5.915	0.169	6.220	1.607	7.755	0.902
	10	**5.135**	**0.580**	**5.575**	**4.484**	**5.910**	**0.338**	**6.280**	**0.955**	**7.730**	**1.293**
	09	NA		5.550	5.765	5.910	0.338	NA		7.735	1.422
L_6	11	5.14	0.778	5.565	4.851	5.914	0.151	NA		7.730	1.293
	10	**5.135**	**0.58**	**5.575**	**4.484**	**5.910**	**0.338**	**6.280**	**0.955**	**7.730**	**1.293**
	9	5.135	0.58	5.585	4.834	5.910	0.338	NA		7.965	0.878
L_7	9.0	5.135	0.584	5.575	4.484	5.760	0.278	6.280	0.955	7.730	1.293
	8.0	**5.135**	**0.584**	**5.575**	**4.484**	**5.910**	**0.338**	**6.280**	**0.955**	**7.730**	**1.293**
	7.0	5.145	0.583	5.570	4.667	6.030	0.331	6.285	0.477	7.730	1.293

Table 3. Summary of results presented in Figure 10.

parameter	Truncation length (mm)	AR1		AR2		AR3		AR4		AR5	
		CF (GHz)	ARBW (%)	CF (GHz)	ARBW (%)	CF (GHz)	ARBW (%)	CF (GHz)	ARBW (%)	CF (GHz)	ARBW (%)
ΔL	7.4	NA		5.665	5.825	NA		6.330	0.947	7.855	0.891
	6.9	**5.135**	**0.58**	**5.575**	**4.484**	**5.910**	**.338**	**6.280**	**0.955**	**7.730**	**1.293**
	6.4	NA		5.580	3.584	6.065	0.164	NA		8.045	0.372

3.3. Effect of Corner Truncation

Figure 10 illustrates the effect of different value of length ΔL of corner truncation of all the three patches on the axial ratio. It is clear from the figure that the variation of truncation length ΔL has the great effect on the CP performances. When decreasing the truncation length ΔL, three CP bands with narrow axial ratio bandwidth have been obtained. Three CP bands are obtained with increasing truncation length ΔL.

Table 3 summarizes the effect on the CF and ARBW of different CP bands of the antenna with variation in the truncation length. The CP bands AR1 and AR3 disappear with increasing the truncation length ΔL, while the CP bands AR1 and AR4 disappear with decreasing the truncation length ΔL. The CF of CP band AR2 shifted downward with increased bandwidth and CF of CP bands AR4 and AR5 shifted upward with an increase in the truncation length ΔL. The CF of CP bands AR2, AR3 and AR5 shifted upward with a decrease in the truncation length ΔL. From the parametric studies, it can

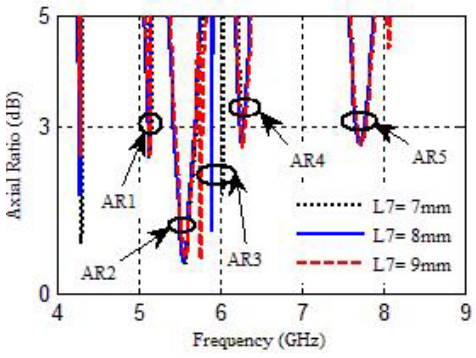

Figure 9. Variation of axial ratio for different value of length L_7 of slot in lower patch.

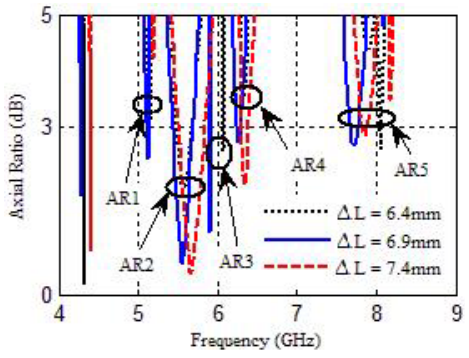

Figure 10. Variation of axial ratio for different value of length ΔL of corner truncation.

Table 4. Optimized design parameter of the proposed antenna. (Values in mm).

L	W	s	t	d	g
15.5	16.4	3.7	1.2	2.12	4.44
h_1	h_2	ΔL	L_1	L_2	L_3
1.56	1.56	6.9	6.74	3.69	4.95
L_4	L_5	L_6	L_7	w	d_1
10	6.0	10	8	1	2.32

be concluded that the length of the slits, slots and corner truncation are the critical parameters and needs serious consideration for the CP performances. Finally, the optimized dimensions of the proposed antenna are listed in Table 4. The proposed antenna can operate in five different CP bands through a design optimization.

4. RESULTS AND DISCUSSIONS

The corner truncation slits cut in upper patch, lower patch and middle patch and embedding slots in the middle and lower patches play an important role in achieving multiband circular polarization. The measured and simulated reflection coefficients of the proposed antenna are presented in Figure 11. The antenna shows wideband characteristics with an impedance bandwidth of 52.13% in the frequency range of 4.85 GHz to 8.27 GHz. A good agreement between simulated and measured result is obtained. The little shift in the bandwidth is observed due to some material impurity and fabrication imperfection. Figure 11 also demonstrates the axial ratio at an angle of 22° from the broadside direction as the maximum radiation takes place in this direction. It is clear at the point of observation that the proposed antenna exhibits five different CP bands in the frequency range of 5.12 GHz to 5.15 GHz (AR1), 5.45 GHz to 5.70 GHz (AR2), 5.90 GHz to 5.92 GHz (AR3), 6.25 GHz to 6.31 GHz (AR4) and 7.68 GHz to 7.78 GHz (AR5) with axial ratio bandwidths of 0.51%, 4.54%, 0.33%, 0.83% and 1.29% respectively. Clearly, good CP performance with an axial ratio less than 3 dB is obtained on all frequency bands. The measured and simulated axial ratios of the CP bands AR1, AR2, AR3 AR4 and AR5 are shown in Figure 12. The measured axial ratio bandwidths are 0.49%, 4.23%, 0.30%, 0.79% and 1.23% and are in good agreement with simulated result. Figure 13 illustrates the simulated and measured gain of the proposed antenna at the point of observation. The simulated gain at the centre frequencies of the various CP bands AR1, AR2, AR3, AR4 and AR5 are 2 dBi, 4 dBi, 5 dBi, 5.5 dBi and 6 dBi respectively. In addition, the comparisons of number of CP bands and number of layers to previously reported CP antennas are presented in Table 5. It is clear that five CP bands are obtained using only three layers of the patches.

The circularly polarized antenna can be categorized as left-hand circular polarized (LHCP) and right-hand circular polarized (RHCP) antennas having opposite radiation property. An antenna made for LHCP reception can not receive RHCP and vice versa like horizontally and vertically polarized antennas. The relative magnitudes of LHCP and RHCP radiation determine the type of antenna.

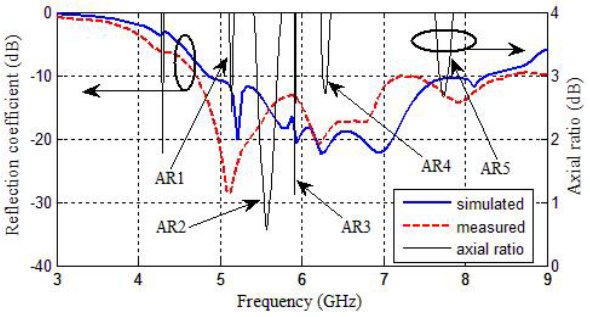

Figure 11. Measured and simulated reflection coefficients and axial ratio of the proposed antenna.

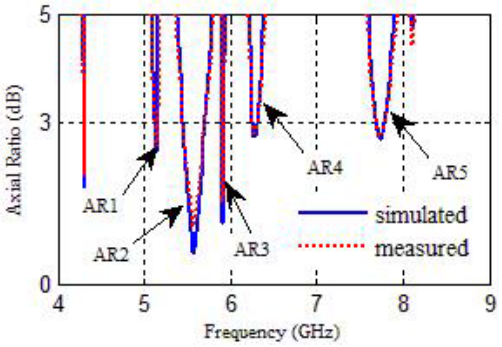

Figure 12. Measured and simulated axial ratios for AR1, AR2, AR3, AR4 and AR5 CP bands.

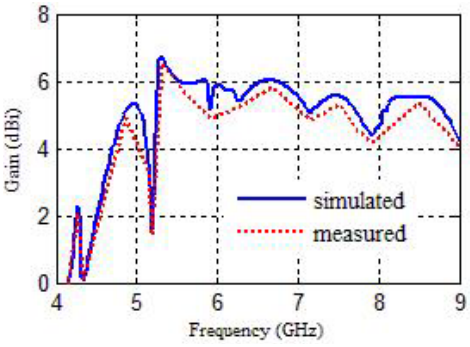

Figure 13. Measured and simulated gains of the proposed antenna.

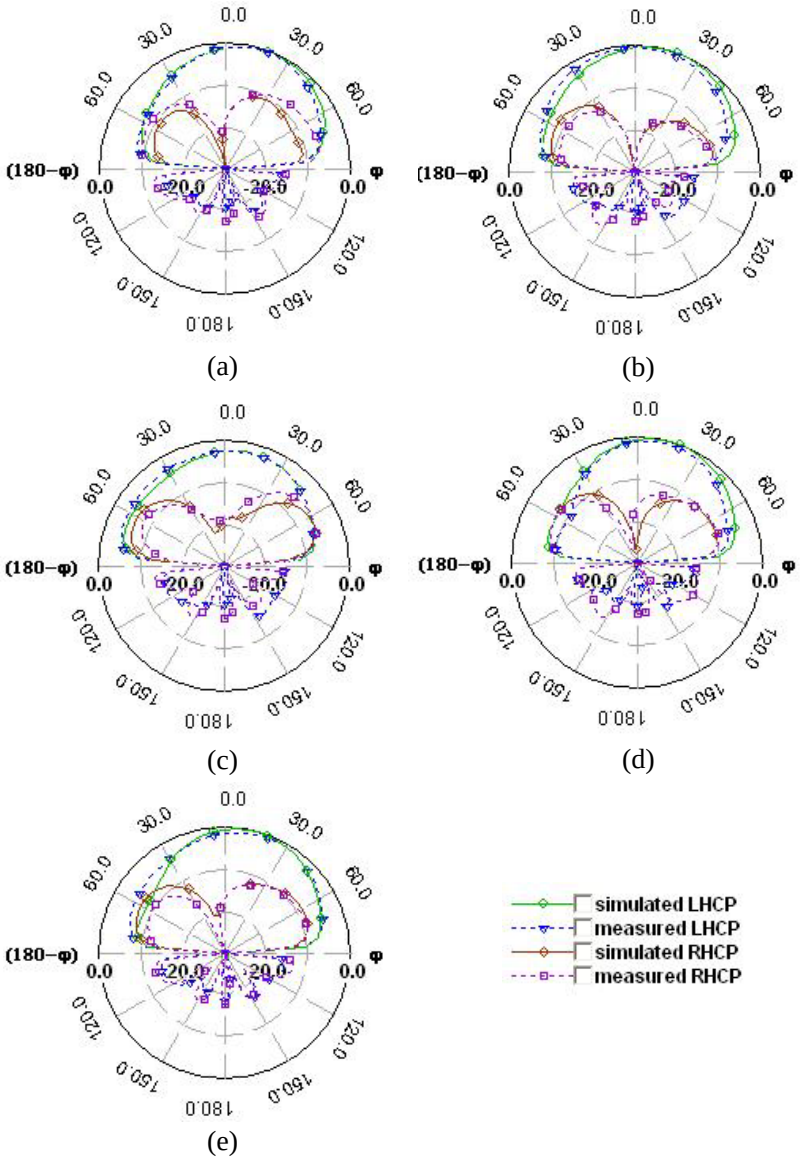

Figure 14. Measured and simulated E-plane ($\Phi = 0°$) left and right circularly polarized radiation patterns at (a) 5.14 GHz, (b) 5.57 GHz, (c) 5.91 GHz, (d) 6.28 GHz, and (e) 7.73 GHz.

Table 5. Comparisons of number of CP bands and number of layers for reporting CP antennas.

References	[6]	[9]	[10]	[11]	[12]	[16]	[17]	[17]	**This work**
Number of CP bands	2	2	2	2	2	3	3	4	**5**
Number of Layers	2	2	2	3	2	2	3	4	**3**
CP per layer	1	1	1	0.67	1	1.5	1	1	**1.67**
Bandwidth of CP Bands (below 3 dB)	3.7% 1.9%	1.76% 2.67%	0.9% 1.0%	1.36% 2.21%	0.4% 1.12%	0.64% 0.93% 0.64%	3.40% 0.81% 0.83%	5.3% 0.7% 0.8% 0.5%	**0.51%** **4.54%** **0.33%** **0.83%** **1.29%**

Figures 14(a), 14(b), 14(c), 14(d) and 14(e) show the simulated and measured E-plane ($\Phi = 0°$) LHCP and RHCP radiation pattern at centre frequencies of AR1, AR2, AR3, AR4 and AR5, i.e., at 5.14 GHz, 5.57 GHz, 5.91 GHz, 6.28 GHz and 7.73 GHz respectively. The figures also make it clear that LHCP is 10 dB more than RHCP for each band and makes the proposed antenna LHCP. It is also noticeable that maximum radiation occurs at around 22° for all the CP bands. That is why the axial ratio was taken at 22°. The discrepancy between measured and simulated radiation patterns is due to the finite ground plane used in the measurement set-up as compared to the infinite ground plane assumed in the simulations. A good amount of axial ratio beam width may be observed from this figure, which determines the angle in which CP radiation is obtained.

5. CONCLUSION

Capacitive coupled stacked microstrip antenna with multiband CP operation is presented and fabricated. The proposed antenna covers a wide impedance bandwidth and operates in five different CP bands. The multiband CP radiation is achieved by proper selection and tuning of corner truncation, slits in the three stacked patches and inclined slots in the middle patch and lower patch. The proposed antenna gives five different CP bands with the axial ratio bandwidth of 0.51%, 4.54%, 0.33%, 0.83% and 1.29%. The antenna is suited for satellite communication, Wi-Fi services in C-band, cordless phones and C-band weather radar systems. The antenna is a good example of antenna useful for multiband CP wireless communication systems.

REFERENCES

1. Pozar, D. M. and S. M. Duffy, "A dual-band circularly polarized aperture-coupled stacked microstrip antenna for global positioning satellite," *IEEE Transactions on Antennas Propagation*, Vol. 45, No. 11, 1618–1625, 1997.
2. Woung, K. L. and T. W. Chiou, "Broadband single patch circularly polarized microstrip antenna with dual capacitively coupled feeds," *IEEE Transactions on Antennas Propagation*, Vol. 49, No. 1, 41–44, 2001.
3. Wu, T., H. Su, L. Gan, H. Chen, J. Huang, and H. Zhang, "A compact and broadband microstrip stacked patch antenna with CP for 2.45-GHz mobile RFID reader," *IEEE Transactions Antennas and Wireless Propagation Letters*, Vol. 12, 623–626, 2013.
4. Gautam, A. K., A. Kunwar, and B. K. Kanaujia, "Circularly polarized arrowhead-shape slotted microstrip antenna," *IEEE Transactions Antennas and Wireless Propagation Letters*, Vol. 13, 471–473, 2014.

5. Heidari, A. A., M. Heyrani, and M. Nakhkash, "A dual band circularly polarised stub loaded microstrip patch antenna for GPS applications," *Progress In Electromagnetics Research*, Vol. 92, 195–208, 2009.
6. Li, Q., F. Zhang, G. Zhang, B. Ang, and M. Liang, "A single feed dual band dual sense circularly polarized microstrip antenna," *Progress In Electromagnetics Research C*, Vol. 51, 27–33, 2014.
7. Yim, H.-Y. A., C.-P. Kong, and K.-K. M. Cheng, "Compact circularly polarized microstrip antenna design for dual band applications," *Electron. Letters*, Vol. 47, No. 7, 1–2, 2006.
8. Pozar, D. M. and S. M. Duffy, "A dual band circularly polarized aperture coupled stacked microstrip antenna for global positioning satellite," *IEEE Transactions on Antennas Propagation*, Vol. 45, No. 11, 1618–1625, 1997.
9. Zakaria, N., S. K. A. Rahim, T. S. Ooi, K. G. Reza Tan, and S. A. A. W. Ranim, "Design of stacked microstrip dual-band circular polarized antenna," *Radio Engineering*, Vol. 21, 875–880, 2012.
10. Lee, H. R., H. K. Ryu, S. Lim, and J. M. Woo, "A miniaturized, dual-band, circularly polarized microstrip antenna for installation into satellite mobile phones," *IEEE Transactions Antennas and Wireless Propagation Letters*, Vol. 8, 823–825, 2009.
11. Sharma, V. and M. M. Sharma, "Dual band circularly polarised modified rectangular patch antenna for wireless communication," *Radio Engineering*, Vol. 23, No. 1, 195–202, 2014.
12. Yuan, H. Y., J. Q. Zhang, S. B. Qu, H. Zhou, J. F. Wang, H. Ma, and Z. Xu, "Dual-band dual-polarised microstrip antenna for compass navigation satellites system," *Progress In Electromagnetics Research C*, Vol. 30, 213–223, 2012.
13. Noghabaei, S. M., S. K. A. Rahim, P. J. Soh, M. Abedian, and G. A. Vandenbosch, "A dual band circularly polarised patch antenna with a novel asymmetric slot for Wi-MAX application," *Radio Engineering*, Vol. 22, No. 1, 291–295, 2013.
14. Rao, B. R., M. A. Smolinski, C. C. Quach, and E. N. Rosario, "Triple band GPS trap-loaded inverted L antenna array," *Microwave and Optical Technology Letters*, Vol. 38, No. 1, 35–37, 2003.
15. Doust, E. G., M. Clenet, V. Hemmati, and J. Wight, "An aperture coupled circularly polarised stacked microstrip antenna for GPS frequency bands L_1, L_2, L_5," *IEEE Transactions Antennas and Propagation Society International Symposium*, 1–4, 2008.
16. Liau, W., Q. Chu, and S. Du, "Tri-band circular polarized stacked microstrip antenna for GPS and CNSS applications," *ICMMT Proceedings*, 252–255, 2010.
17. Falade, O. P., M. U. Rehman, Y. Gao, X. D. Chen, and C. G. Parini, "Single feed stacked circular polarised antenna for triple band operation," *IEEE Transactions on Antennas Propagation*, Vol. 60, No. 10, 4479–4484, 2012.
18. Falade, O. P., X. Chen, Y. Alfadhi, and C. Parini, "Quad band circular polarised antenna," *Antennas and Propagation Conference (LAPC)*, 1–4, 2012.